AUTOMATIC CORONARY EXTRACTION BY SUPERVISED DETECTION AND SHAPE MATCHING

Yoshiro Kitamura, Yuanzhong Li, Wataru Ito

Imaging Technology Center, FUJIFILM corporation, Tokyo, JAPAN

ABSTRACT

Automatic coronary extraction has great clinical importance in the effective handling and visualization of large amounts of 3D data. Despite tremendous previous research, coronary extraction remains difficult. Two such difficulties are extraction of both normal and abnormal vessels and reconstruction of exact tree structures based on anatomical knowledge.

To solve the first difficulty, we propose a method to learn a classifier of a tubular 3D object with a dimension reduction approach using Hessian analysis. This enables detection of vessel candidate points despite variations in their appearances. Regarding the second difficulty, we propose an approach to apply the MRF framework for vascular structure segmentation. A novelty of the approach is incorporating constraints to avoid topological inconsistency. Correspondences between the candidate points and model points are found using a graph matching process during which, tree structures as per the shape model are simultaneously reconstructed. Experimental results show robustness of the method. The proposed method can improve clinical workflow.

Index Terms— Vascular structure segmentation, Machine learning, Shape matching

1. INTRODUCTION

Cardiac diseases are the major causes of death in developed countries. Because 3D CT angiography is a standard examination for the diseases, automatic coronary extraction from CT data has great clinical importance for effectively handling and visualizing large amounts of 3D data.

The main purpose of coronary extraction is to reconstruct a graph structure of the coronary artery centerline. Despite the tremendous amount of past studies on the subject as reviewed in [1], coronary extraction remains a challenging task. Two of the major difficulties of this process are that the normal as well as abnormal vessels must be extracted and the coronary artery tree should be reconstructed on the basis of anatomical knowledge.

Regarding the first difficulty, popular tubular structure detection approaches such as Hessian filtering [2] often fail to detect abnormal vessels (e.g., soft plaques, hard plaques, or stent grafts) since their appearances have insufficient contrast or different image patterns. Machine learning was applied to improve detection performance [3]. However the benefit of the learning is limited since it learns classifiers in low dimensional feature spaces. Other improved vesselness measures have been proposed based on gradient vector flow [4] and ray casting [5].

Regarding the second difficulty, since coronary veins or pulmonary vessels sometimes intersect arteries, general spanning tree algorithms are hard to discriminate arteries from the other vessels [6]. As a result, the extracted graphs often have incorrect tree structures or extra branches. Utilizing branch-level information decreases these failures [4,5]. In cases where the start and end points of a vessel are given, minimal path approaches [7] are robust even in cases of severe anomalies. While tracking-type methods [8] are prone to halting prematurely in the presence of anomalies, an interactive method based on multiple hypothesis tracking was recently proposed to solve these difficulties [9].

In this paper, we propose a novel method that solves the above-mentioned difficulties without any user interaction. This framework is similar to that described in [10,11]. However, since their purpose is not tree reconstruction, topological inconsistency has not been considered.

2. METHODS

The proposed method consists of a candidate detection step and a graph reconstruction step. The challenge of the candidate detection step is detecting vessels despite variations in their appearances. Machine learning is a possible solution for building such a complex appearance model. However, general 3D objects have appearances that are too dispersed for learning. Therefore, we propose a dimension reduction approach for 3D tubular structures by using Hessian analysis.

The other challenge is how to incorporate anatomical knowledge into graph reconstruction. A problem is that vascular shape and topology vary substantially between patients. To tackle this, we propose an approach to decompose the variation into global shape and local topology. The shape is modeled as unary and pairwise distributions. And the local topology is tracked by the minimal path approach. The two components are simultaneously optimized in a graph matching method.

2.1. Candidate detection

This step detects all vessel candidate points within a target volume. To detect various size of vessel, multi-scale exhaustive search is done. At each search position, an orientation of the object is estimated. Then the object is classified whether a vessel or non-vessel.

2.1.1. Orientation estimation

The orientation of the object is estimated using Hessian analysis [2]. A Hessian matrix is a matrix of second-order partial derivatives. We can extract three orthogonal directions in the order of the strength of the second derivatives by eigenvalue decomposition. The eigenvector corresponding to the smallest eigenvalue is the orientation of the object.

2.1.2. Vessel classification

The object is classified as a vessel or non-vessel on the basis of its appearance. We used AdaBoost for learning a classifier [12], since it has the advantage of realizing fast detection with a cascade structure.

The classifier is learned as follows. Positive training samples are prepared from training data by manually labeling centerlines and vessel contours. To make a classifier that can discriminate abnormal vessels as the vessel class, the abnormal vessels are included in the positive samples. All positive samples are normalized to its orientation and radius (Fig. 1). Negative training samples are chosen randomly at first and then added using the bootstrap technique.

AdaBoost learns a classifier that discriminates the positive and negative samples by sequentially combining the feature vectors. We extracted the feature vectors using Haar-like filtering [13]. Each vector is a quantized value of intensity differences in two neighboring rectangular regions. In our implementation, the normalized image was set as 10^3 voxels. The sizes of the rectangular regions were ranged 1^3 to 4^3 voxels. The vessel classifier was learned from 200,000 samples extracted from 10 training data.

At testing, the heart regions of target data were rescaled to be 0.5-mm isotropic voxels. Exhaustive search was applied for five scales of Gaussian pyramid images which were generated from the rescaled image by down-sampling from 0.5 to 2.0-mm/voxel by a factor of $\sqrt{2}$ steps. For the orientation estimation, we used a Gaussian kernel with σ = 1.0 (voxel). The size σ corresponds to the radius and the smallest eigenvector corresponds to the orientation of the image normalization.

2.2. Graph reconstruction

This step reconstructs coronary tree structures by connecting the candidate points. We explain the shape model, matching method, and energy function used for the matching.

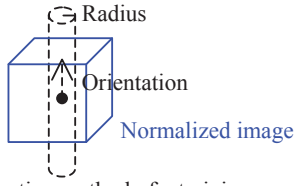


Figure 1: Normalization method of a training sample.

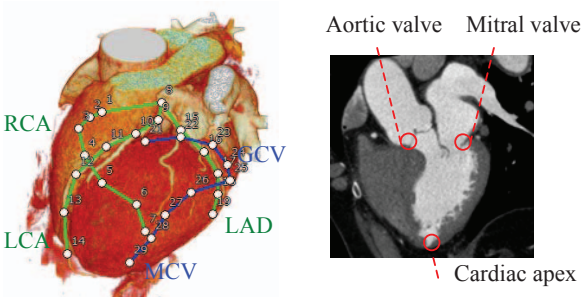


Figure 2: (Left) Coronary artery/vein model of discrete points. The artery and vein points are connected with green and blue lines, respectively. (Right) Three cardiac feature points on a MPR image to normalize coordinate system.

2.2.1. Shape model

We defined a shape model of coronary vessels as 30 discrete nodes (each node has its own index: q) and 28 edges that connect a specific node pair (Fig. 2 (Left)). This model represents three main coronary arteries and two coronary veins.

The model is given probability distributions learned from training data in which the correct node positions have been labeled. We denote a probability when q' is assigned in the following 3D coordinate of a point p': $X_{p'}$ as $S_{q'}(X_{p'})$. Each distribution of the node position is approximated by a simple Gaussian function as: $S_{q'}(X_{p'}) = N\left(X_{p'} \mid \mu_{q'}, \sigma_{q'}^2\right)$. Where $\mu_{q'}$ and $\sigma_{q'}$ are the mean position and standard deviation of the distribution of q', respectively. We denote a probability when a node pair (q', q'') is assigned 3D coordinates ($X_{p'}$, $X_{p''}$), as $S_{q'q''}(X_{p'}, X_{p''})$. This is given by a similar formula with a mean position, $\mu_{q'q''}$, and a standard deviation, $\sigma_{q'q''}$, of the differential distribution of positions q' and q'': $S_{q'q''}(X_{p'}, X_{p''}) = N\left(X_{p'} - X_{p''} \mid \mu_{q'q''}, \sigma_{q'q''}^2\right)$. For verification tests, the probability distributions were learned from 20 training data.

Note that we transform the coordinate system before the probability computation. Three landmarks are detected by applying AdaBoost detectors on multi-planar reconstruction images (Fig. 2 (Right)) [14]. After detecting the landmarks from each data, the 3D coordinates are normalized by shift, scale, and rotation.

2.2.2. Graph matching

We solved a graph matching problem to match the model [10,15]. Let us denote P and Q as the sets of points from the object and model. $R \subseteq P \times Q$ denotes the set of potential correspondences. We define the Boolean indicator variable

$$x_{p,q} = \begin{cases} 1 & if\ (p,q) \in R\ is\ a\ correspondence \\ 0 & otherwise \end{cases} \quad (1)$$

In this paper, we consider matching problems under a requirement known as the uniqueness constraint. Thus, we have the set of feasible solutions defined as:

$$C = \{x \in \{0,1\}^{P \times Q} \mid \sum_{p \in P} x_{p,q} \le 1, \sum_{q \in Q} x_{p,q} \le 1, \quad \forall\, p \in P \text{ and } \forall\, q \in Q\}. \quad (2)$$

We define an energy function $E(x)$ with unary and pairwise potentials. The goal is to find the configuration $x \in C$ minimizing $E(x)$.

$$\min_{x \in C} E(x \mid \theta) = \sum_{a \in R} \theta_a x_a + \sum_{(a,b) \in R \times R} \theta_{ab} x_a x_b \quad (3)$$

For correspondences $a=(p',q')$ and $b=(p'',q'')$, θ_a is the matching cost for each correspondence $a \in R$ and θ_{ab} for a pair of correspondences $(a,b) \in R \times R$. We applied dual decomposition (DD) method to minimize the function. The DD method decomposes the main problem into multiple small subproblems which are convex combinations. So the function can be minimized using a projected subgradient method. We decomposed the problem in a similar manner as the local subproblem described in [15]. For each node, we create one subproblem involving only the target node and neighbor nodes connected by the edges. A solution for each subproblem is found with a branch-and-bound method.

2.2.3. Energy function with topology constraint

We designed the energy function as follows:

$$\theta_a = -S_{q'}(X_{p'}) \quad (4)$$

$$\theta_{ab} = -S_{q'q''}(X_{p'}, X_{p''}) + T_{q'q''}(p', p'') \quad (5)$$

$S_{q'}$ and $S_{q'q''}$ measure how much the object node matches the model shape. $T_{q'q''}$ is a topological condition regarding the paths to be reconstructed. That is represented as:

$$T_{q'q''}(p', p'') = \min_{(p''', p'''') \in Path(p', p'')} \sum e_{local}(p''', p'''') \quad (6)$$

Here e_{local} represents the energy between each pair of the object nodes; it has a smaller value if a pair has closer positions, and similar intensities, directions and radii. $\min \sum_{\in Path(p', p'')}$ represents the minimum cost path of all possible paths from p' to p''. Therefore, this term adds a penalty value if an appropriate path does not exist (Fig. 3). The energy function works for the correspondences to be assigned on a straight and continuously extending path along the model. To compute θ_{ab}, the shortest path problem of pairs is solved using the Dijkstra method.

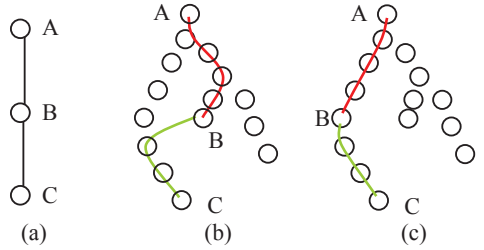


Figure 3: Examples of shape matching. (a) is an assumed model. The topology term takes a large penalty value when the correspondence is assigned to different branches (b), in comparison to the same branch (c).

2.3. Post-processing

Since our goal is to extract entire artery trees, artery branches not included in the model are connected as follows. First, edges with the minimum costs are prepared along the matched artery paths. Other possible edges are prepared with costs calculated from the pairs of node positions, directions, radii and intensities. Two nodes matched as left and right artery origins are set as seeds. Then minimum spanning tree (MST) algorithm grows trees in the order of the costs, while edges having high costs are rejected. The matched vein paths as well as the other candidate points that have not been connected to the main arteries are removed.

Finally, centerline refinement process is adopted to improve the accuracy of the centerlines. To detect vessel contours, 3D curved planar reconstructed (CPR) images along every extracted branches are generated. Foreground (lumen) and background intensities are estimated based on the radii. The contours are found as Min-cuts planes having closer value to the middle of the estimated intensities [16]. Refined centerlines are generated as the average of the detected contours.

3. EXPERIMENTS

First, we briefly show the impacts of the proposed method. Fig. 4 shows candidate detection results obtained by a conventional Hessian detector, and the proposed method. Here the Hessian detector classifies vessel by thresholding the vesselness measure calculated from the Hessian matrix [2]. The Hessian detector failed to detect vessels with severe plaques, while the AdaBoost detector succeeded.

Fig. 5 shows graph reconstruction results obtained by a conventional method and the proposed method. The conventional method utilizes the MST algorithm to generate trees from the candidate points [6]. A problem in the graph reconstruction is that large gaps exist due to motion artifacts or miss-detection of the candidate points. The MST based method depends on a parameter specifying the distance allowed for connecting points. Longer allowed distances result in greater numbers of true and false branches. However the proposed method is able to connect branches across such gaps, because of the shape prior. Note that we used our original CTA data for training of the algorithm.

Next, the proposed method was evaluated with the Rotterdam Coronary Artery Algorithm Evaluation Framework [17]. In this framework, 32 coronary CTA datasets were arranged. Four coronary branches (RCA, LAD, LCX and one large side-branch) per dataset were manually

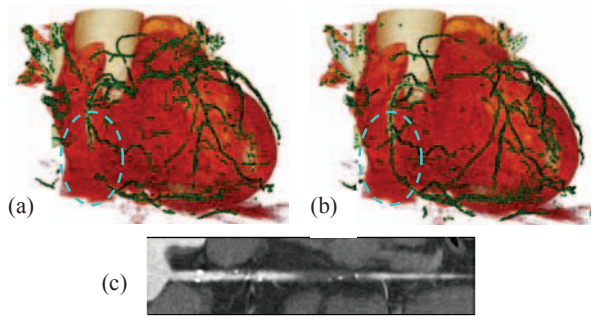


Figure 4: Candidate detection results obtained from (a) the Hessian detector and (b) the AdaBoost detector. (c) a CPR image of the vessel with a severe plaque in the circled area. The green dots represent detected points.

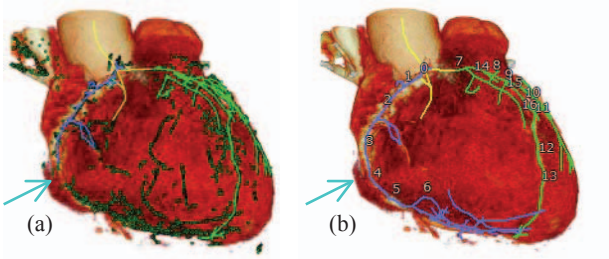


Figure 5: Tree reconstruction results obtained with (a) the conventional method and (b) the proposed method. The indexes shown in (b) represent positions where the model points were assigned. The indexes were assigned across the gap at the arrow.

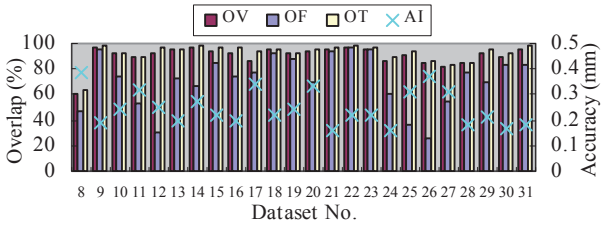


Figure 6: Evaluation results from RCAA evaluation framework.

annotated by three experts. All branches for evaluation were automatically selected based on reference points provided by the framework. Then the algorithm was evaluated by comparing the extracted centerlines with the reference standard in two aspects: extraction ability and accuracy. The extraction ability is measured by three overlap values, which are overall overlap (OV), overlap until first error (OF) and overlap with the clinically relevant part (OT). The accuracy is measured as average distance to the reference centerlines.

The evaluation results of testing datasets (No.8–31) are summarized in Fig. 6. The average measurements are OV = 90.6%, OF = 70.9%, OT = 92.5% and AI = 0.25mm. The average processing time per dataset was 40.4 seconds with a parallelized implementation on a quad-core 2.8 GHz PC. The performance is better than of a human user on most datasets. Compared with the 5 automatic methods presented at the MICCAI 2008 workshop [17], the overlap measurements of the proposed method is ranked 2nd position, and the accuracy is ranked 1st position.

Regarding the extraction ability, major failures were occurred in LAD and LCX because individual variations in branching and positioning were bigger than in RCA. Including side branches to the shape model will improve the overlap rates. Most minor failures occurred near the end of vessels having unclear image contrast.

4. CONCLUSION

We proposed a novel method for automatic coronary extraction from 3D CT angiography. The experimental results demonstrated robustness of the method. The proposed method can improve clinical workflow.

5. REFERENCES

[1] D. Lesage *et al*. A review of 3D vessel lumen segmentation techniques: models, features and extraction schemes. *Medical Image Analysis*, 13(6):819–845, 2009.

[2] A. F. Frangi *et al*. Multiscale vessel enhancement filtering, *Proc. of MICCAI*, 130–137, 1998.

[3] A. Santamaria-Pang *et al*. Automatic centerline extraction of irregular tubular structures using probability volumes from multiphoton imaging, *Proc. of MICCAI*, 2:486–494, 2007.

[4] C. Bauer and H. Bischof. Edge Based Tube Detection for Coronary Artery Centerline Extraction, *In MICCAI 2008 Workshop Proceedings, 2008*.

[5] G. Yang *et al*. Automatic centerline extraction of coronary arteries in coronary computed tomographic angiography, *Int. J Cardiovascular Imaging*, 2011.

[6] A. Szymczak *et al*. Coronary vessel trees from 3D imagery: A topological approach. *Medical Image Analysis*, 10:548–559, 2006.

[7] D. Lesage *et al*. Bayesian maximal paths for coronary artery segmentation from 3D CT angiograms. *Proc. of MICCAI*, 1:222–229, 2009.

[8] G. Lavi *et al*. Single-seeded coronary artery tracking in CT angiography. *Nuclear Science Symposium Conference Record, IEEE*, 5:3308–3311, 2004.

[9] O. Friman *et al*. Multiple hypothesis template tracking of small 3D vessel structures. *Medical Image Analysis*, 14(2):160-171, 2010.

[10] C. Wang *et al*. 3D knowledge-based segmentation using pose-invariant higher-order graphs. *Proc. of MICCAI*, 3:189–196, 2010.

[11] R. Donner *et al*, Sparce MRF appearance models for fast anatomical structure localization, *In BMVC*, 2007.

[12] J. Friedman *et al*. Additive logistic regression: a statistical view of boosting (with discussion and rejoinder by the authors). *Annals of Statistics*, 28(2), 337–407, 2000.

[13] P. Viola and M. Jones. Rapid object detection using boosted cascade of simple features, *Proc. of CVPR*, 1:511–518, 2001.

[14] C. Wang *et al*. A machine learning approach to extract spinal column centerline from three-dimensional CT data. *Proc. of SPIE MI*, 72594T, 2009.

[15] L. Torresani, V. Kolmogorov, and C. Rother. Feature correspondence via graph matching: Models and global optimization. *In ECCV*, 596–609, 2008.

[16] Y. Boykov and V. Kolmogorov, An Experimental Comparison of Min-Cut/Max-Flow Algorithms for Energy Minimization in Vision, *IEEE PAMI*, 26(9), 1124-1137, 2004.

[17] M. Schaap, C. Metz, *et al*., Standardized Evaluation Methodology and Reference Database for Evaluating Coronary Artery Centerline Extraction Algorithms, *Medical Image Analysis*, 2009.